Materials Science Forum
ISSN: 1662-9752, Vol. 930, pp 637-642
doi:10.4028/www.scientific.net/MSF.930.637

Submitted: 2018-01-17
Accepted: 2018-01-24
Online: 2018-09-14

Effect of Hydrogen Decrepitation Pressure on the Particle Size of Rare Earth Based Alloys for Ni-MH Battery Production

Edson Pereira Soares[1], Julio Cesar Serafim Casini[2,*], Ligia Silverio Vieira[2], Franks Martins Silva[2], Rubens Nunes de Faria[1], Hidetoshi Takiishi[1]

[1]Materials Science and Technology Center - CCTM, Nuclear and Energy Research Institute - IPEN, University of São Paulo - USP, SP 05508-900, Brazil.

[2]Federal Institute of Education, Science and Technology of Rondônia Campus Calama - IFRO, RO 76820-441, Brazil. RO, Brazil.

*epsoares@ipen.br

*Corresponding Author: julio.casini@ifro.edu.br
Av. Calama, 4985, Flodoaldo Pontes Pinto, 76820-441, Porto Velho, Rondonia

Keywords: rare earth, transition metal, microanalyses, battery, decrepitation.

Abstract: This paper presents the results obtained from the hydrogenation and decrepitation of three LaNi-based alloys, $La_{0.7}Mg_{0.3}Al_{0.3}Mn_{0.4}Co_{0.5}Ni_{3.8}$, $La_{0.7}Mg_{0.3}Al_{0.3}Mn_{0.4}Cu_{0.5}Ni_{3.8}$ and $La_{0.7}Mg_{0.3}Al_{0.3}Mn_{0.4}Sn_{0.5}Ni_{3.8}$, in the as-cast condition. The procedure for decrepitating the alloys to be used in the negative electrode of the batteries was carried out using a combination of various hydrogen pressures (2-9 bar) at room temperature. At 2 bar of H_2 it was revealed that Co, Cu and Sn have influence on the microstructures of the hydrogenated alloys and on the efficiency of hydrogen decrepitation. None of these alloys required thermal heating to activate and start the hydrogen absorption process. The decrepitated materials were characterized by scanning electron microscopy (SEM). The electrochemical measurements were performed using the tested negative electrode between two $Ni(OH)_2$ electrodes as a battery cell.

Introduction

Since the beginning of $LaNi_5$-based alloys development for hydrogen storage, many investigations have been conducted to analyze the effect of elemental substitutions on the base alloy [1-8]. The purpose of the modifications is to improve the negative electrode performance of the batteries [9-17]. It has been reported that alloy electrodes produced using hydrogen decrepitation had their activation faster than electrodes prepared by mechanical milling [13]. This study deals with and reports the results of a more detailed investigation carried out on the development of a hydrogen decrepitation procedure to replace the mechanical grinding of ingots of some alloys for negative electrodes represented by the formulae: $La_{0.7}Mg_{0.3}Al_{0.3}Mn_{0.4}Co_{0.5}Ni_{3.8}$, $La_{0.7}Mg_{0.3}Al_{0.3}Mn_{0.4}Cu_{0.5}Ni_{3.8}$ and $La_{0.7}Mg_{0.3}Al_{0.3}Mn_{0.4}Sn_{0.5}Ni_{3.8}$. The material decrepitated by hydrogen has been investigated using a scanning electron microscope. The maximum storage capacity of the alloys was also determined using a battery cycler [18].

Experimental

Commercially available alloys were investigated in the as-cast state (as received condition). The induction melt Ingots were prepared in rectangular copper mold and fast cooled. In order to hydrogenate the cast ingot alloys the following procedure was adopted. Lumps of the alloy (3 g) were cleaned in acetone and manually broken in small pieces (<5 mm). This material was placed in a hydrogenation inconel vessel which was evacuated to backing-pump pressure for 30 min. Hydrogen was then introduced into the inconel vessel. Hydrogen absorption and decrepitation of the alloys was carried out at room temperature at various starting pressure (P_i 2-9 bar) for 60 min. Pressure variation was recorded digitally in mbar for improving data precision. The decrepitated structures of the resulting material were examined using a scanning electron microscope with

energy dispersive X-ray analysis facility. The amount of hydrogen absorbed in the alloy, expressed as the number of atoms of H (n) per unit of formula, calculated from the maximum storage capacity (C_{max}) [2,3] using equation 1:

$$n = \frac{3600}{9.65 \times 10^{7}} Mw \times C\max \quad (1)$$

where M_w is the molecular weight of the alloy and C_{max} is in units of $mAhg^{-1}$.

For the assembly of the negative electrodes were used the sieved alloy (<75μm), nickel powder and PVDF. The negative eletrode manufacturing step consists in mixing these three materials in an agate mortar for 30 minutes. In the next stage, for homogenization, approximately two drops of N-methyl-2-pyrrolidone (NMP) are added using a syringe. This solvent acts on the dissolution of the polyvinylidene fluoride (PVDF) aiding in the pressing of the material, as well as preventing the dissolution of the electrode during the loading and unloading cycles. The electrode assembly was then completed with the uniaxial pressing (3 t) of this mixture in a nickel screen measuring 1x1 cm and then drying in an oven at 100 ° C for 1 h. The positive electrode manufacturing step consists of mixing $Ni(OH)_2$, nickel powder and PVDF with the same steps as described previously for the cathode manufacturing process. Mounting was carried out using two positive electrodes on each side of the tested negative electrode.

Results and Discussion

Table 1 gives the hydrogen pressure variation (ΔP) for the Co-substituted alloys at room temperature (RT) and the number of hydrogen atoms (n) calculated from electrochemically measured C_{max}. A maximum of 4,7 H/f.u. was achieved for the $La_{0.7}Mg_{0.3}Al_{0.3}Mn_{0.4}Co_{0.5}Ni_{3.8}$ alloy. Cu and Sn substitution alloys did not exhibit the same hydrogen uptakes in this processing condition. Figure 1 shows the portions of hydrogen pressure versus absorption time for the alloys at the pressures of 9, 6, 4 and 2 bar of hydrogen processed at ambient temperature.

Table 1. Absorption parameters of hydrogenated alloys and number of hydrogen atoms per unit formula determined using the measured electrochemical capacity.

Elements	C_{max} [$mAh.g^{-1}$]	Mw [$gmol^{-1}$]	n[H/f.u.]
$Co_{0.5}$	326	387	4.7
$Cu_{0.5}$	280	389	4.0
$Sn_{0.5}$	248	417	3.9

Table 2 show the variation of the hydrogen pressure at room temperature for the Co, Cu and Sn alloys. Clearly, the higher substitutions of Co and Cu are favorable to the absorption of hydrogen from these alloys from negative electrodes to nickel hydride batteries. Figure 1 shows the hydrogen pressure plots versus absorption time at room temperature for the alloys. These curve profiles show that the hydrogen absorption behavior changes with the introduction of these elements into the alloy. The pressure variation is lower in the alloy containing Sn, with less hydrogen absorption. Alloys with Cu content showed good absorption of hydrogen in this processing condition [16,18].

Table 2. Parameters of the hydrogen pressure variation absorbed by the alloys.

Elements	$P_{Initial}$	P_{empty}*	P_{end}	$P_{Absorbed}$
$Co_{0.5}$	9000 6000 4000 2000	8420 5940 3750 1970	6110 3670 1560 460	2310 2270 2190 1510
$Cu_{0.5}$	9000 6000 4000 2000	8420 5940 3750 1970	4730 3580 2030 580	3690 2360 1720 1390
$Sn_{0.5}$	9000 6000 4000 2000	8420 5940 3750 1970	7590 4190 2030 940	830 1750 1720 1030

* P_{empty} is the pressure variation in the system without sample in the testing period of time (60 minutes).

The equivalence between gas and electrochemical absorption has been reported by Cuevas et al. [2]. According to this work, for an alloy absorb a quantity of hydrogen by solid-gas reaction an equivalent electrochemical capacity can be calculated according to the Faraday equation. However, actual electrochemical charge is constrained in open cells by the atmospheric pressure, whereas discharge is limited by corrosion potential of the alloy in conjunction with kinetics and polarizations effects. Hence, reversible electrochemical capacities correspond, at the most, to the hydrogen content loaded by the solid-gas method within the pressure range of about 0.01 to 1 bar. It has also been reported in this work that the $LaNi_5$ alloy is can readily and reversibly absorb 6 H/f.u. at room temperature under an equilibrium pressure of about 2 bar [2]. As observed in the present work, the amount of the additive elements is preponderant on the capacity of LaNi-based alloys to absorb hydrogen.

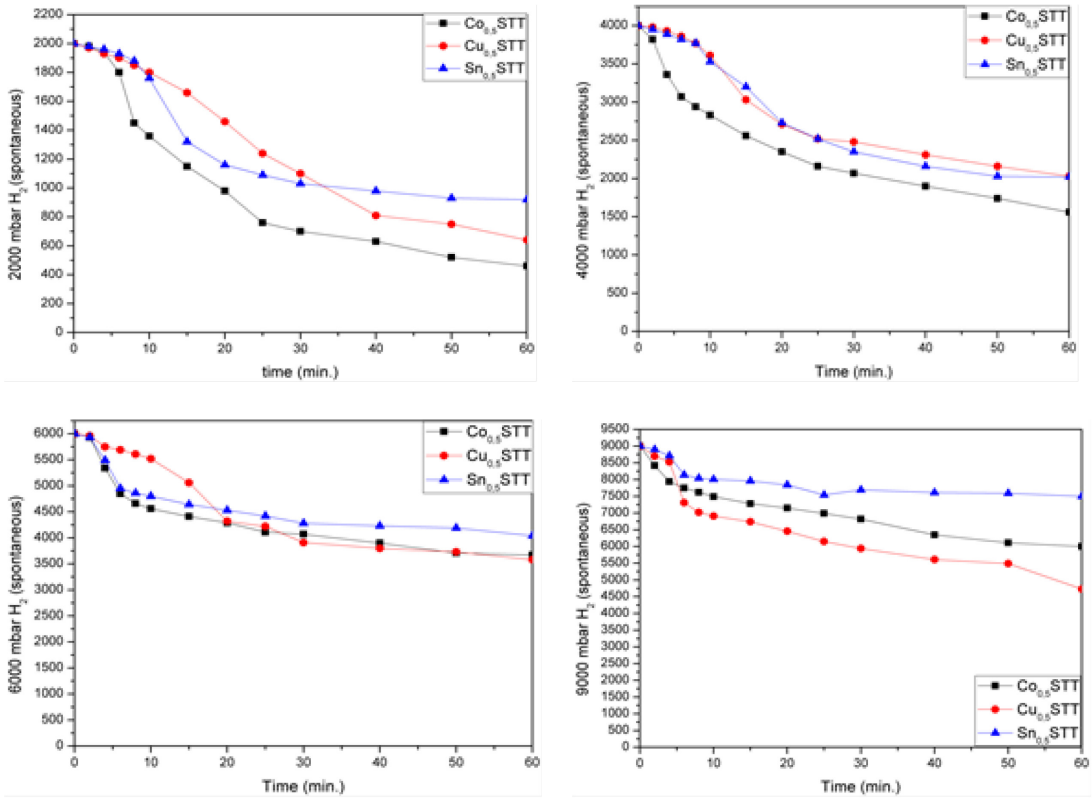

Fig. 1. Hydrogenation curves of the $La_{0.7}Mg_{0.3}Al_{0.3}Mn_{0.4}Co_{0.5}Ni_{3.8}$, $La_{0.7}Mg_{0.3}Al_{0.3}Mn_{0.4}Cu_{0.5}Ni_{3.8}$ and $La_{0.7}Mg_{0.3}Al_{0.3}Mn_{0.4}Sn_{0.5}Ni_{3.8}$ cast ingot alloys.

The structure of the decrepitated alloys can be seen in figure 2 where the pressure of 2 bar of hydrogen was used at room temperature. Previous studies have shown the identification of phases using X-ray diffraction and phase analysis showed that the alloys are composed of a matrix phase ($LaNi_5$), a gray phase (La (Mg) Ni_3) and a dark phase ($MgNi_2$) [15,16,18]. All these microstructural and phase changes may also have some influence on the hydrogen decrepitating behavior observed in this study.

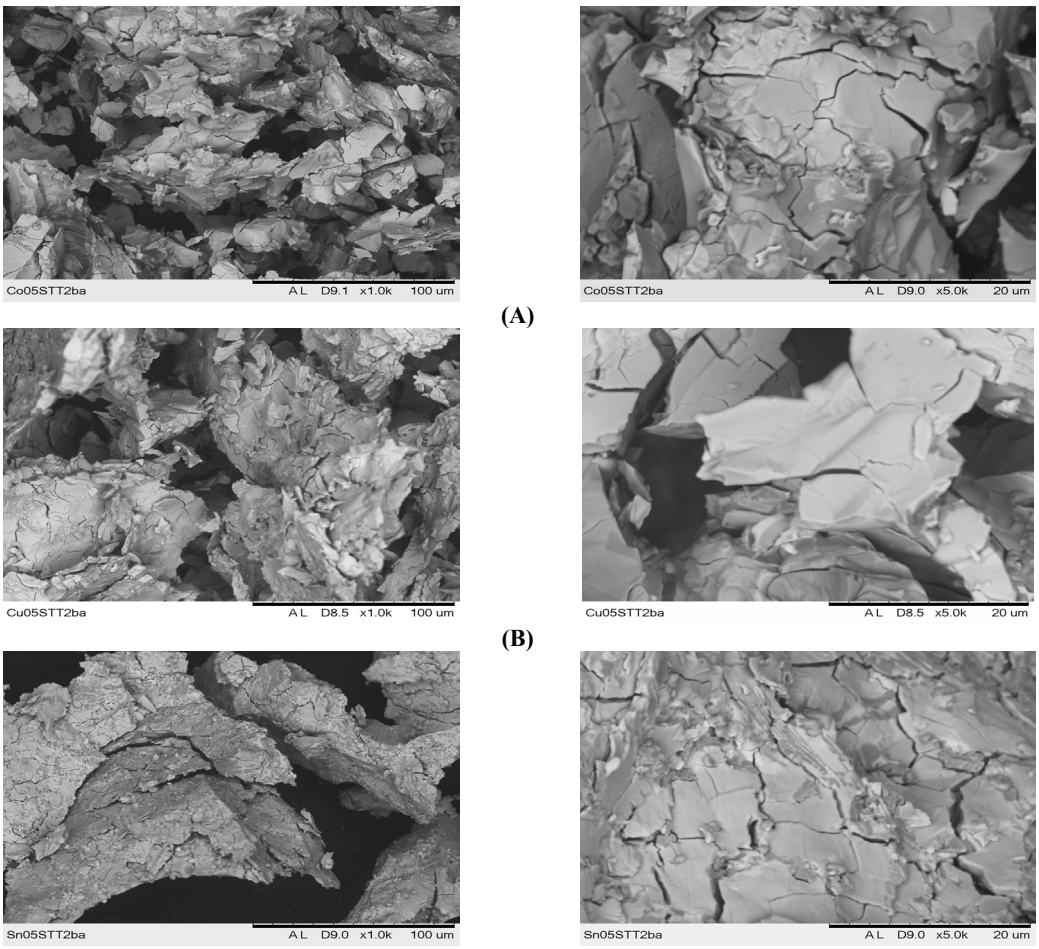

Fig. 2. Electron microscopy images of general and detailed scans of the microstructures of the $La_{0.7}Mg_{0.3}Al_{0.3}Mn_{0.4}Co_{0.5}Ni_{3.8}$ (**A**), $La_{0.7}Mg_{0.3}Al_{0.3}Mn_{0.4}Cu_{0.5}Ni_{3.8}$ (**B**) and $La_{0.7}Mg_{0.3}Al_{0.3}Mn_{0.4}Sn_{0.5}Ni_{3.8}$ (**C**) pulverized in 2 bar of hydrogen at room temperature.

The electrochemical behavior was found to be in good agreement with the hydrogen absorption characteristics of these alloys. Comparatively, the substitution of Co by Cu and Sn decreased more significantly the electrochemical capacity of the alloys as shown in figure 3. The best discharge capacity achieved in these alloys (326 $mAhg^{-1}$) was for the alloy with addition of Co ($La_{0.7}Mg_{0.3}Al_{0.3}Mn_{0.4}Co_{0.5}Ni_{3.8}$).

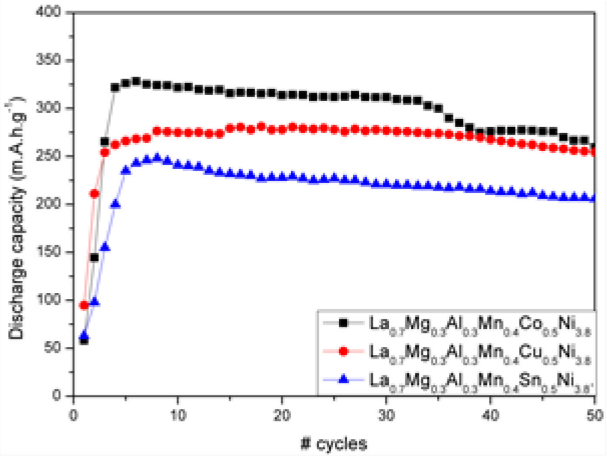

Fig. 3. Discharge capacity curves as a function of the number of cycles of the batteries produced with $La_{0.7}Mg_{0.3}Al_{0.3}Mn_{0.4}Co_{0.5}Ni_{3.8}$, $La_{0.7}Mg_{0.3}Al_{0.3}Mn_{0.4}Cu_{0.5}Ni_{3.8}$ and $La_{0.7}Mg_{0.3}Al_{0.3}Mn_{0.4}Sn_{0.5}Ni_{3.8}$ cast alloys.

Conclusions

The presence of Co, Cu and Sn had a significant effect on the hydrogenation / decrepitation behavior of the LaNi-based hydrogen storage alloys. The decrepitating process was less effective in the case of addition of Sn. This has been partially attributed to the changes in the phases present in the alloy where the electrochemical analysis where exhibited a lower discharge capacity (248 $mAhg^{-1}$). A maximum of 4.7 H / f.u. was estimated for the $La_{0.7}Mg_{0.3}Al_{0.3}Mn_{0.4}Co_{0.5}Ni_{3.8}$ alloy. For the all substituted alloys the hydrogen decrepitation at room temperature was very efficient using a considerably low hydrogen pressure of 2 bar.

Acknowledgements

The authors wish to thank FAPESP, CNPq and IPEN-CNEN/SP for the financial support and infrastructure made available to carry out this investigation.

References

[1] Hongmei, L. Guoxun, Z.Chuanhua, W. Ruikun: Journal of Power Sources Vol. 77 (1999), p.123.

[2] J.J. Reilly, G.D. Adzic, J.R. Johnson, T. Vogt, S. Mukerjee, J. McBreen: J. Alloys and Compounds Vols. 293-295 (1999), p. 569

[3] F. Cuevas, J.M. Joubert, M. Latroche, A. Percheron-Guegan: Applied Physics A Mat. Sc. and Processing Vol. 72 (2001), p. 225.

[4] F. Feng, M. Geng, D.O. Northwood, International Journal of Hydrogen Energy Vol. 26 (7) (2001), p. 725

[5] A. K. Shukla, S. Venugopalan, B. Hariprakash, Journal of Power Sources Vol. 100 (1-2) (2001), p.125.

[6] K. Hong: Journal of Alloys and Compounds Vol. 321 (2) (2001), p. 307.

[7] R.C. Ambrosio, E.A. Ticianelli: Journal of Power Sources Vol. 110 (1) (2002), p. 73.

[8] K. Kadir, D. Noreus, I. Yamashita: Journal Alloys and Compounds Vol. 345 (1-2) (2002), p.140.

[9] I. P. Jain, M. I. S. Abu Dakka: International Journal of Hydrogen Energy Vol. 27 (4) (2002), p.395.

[10] H. Ye, Y.X. Huang, T.S. Huang, H. Zhang: Journal of Alloys and Compounds Vols. 330-332 (2002), p. 866.

[11] Y. Liu, H. Pan, M. Gao, Y. Zhu, Y. Lei, Q. Wang: International J. of Hydrogen Energy Vol. 29 (3) (2004), p. 297.

[12] H. Pan, Q. Jin, M. Gao, Y. Liu, R. Li, Y. Lei: Journal of Alloys and Compounds Vol. 373 (2004), p. 237.

[13] H. Pan, N. Chen, M. Gao, R. Li, Y. Lei, Q. Wang: Journal Alloys and Compounds Vol. 397 (1-2) (2005), p. 306.

[14] H. Pan, X. Wu, M. Gao, N. Chen, Y. Yue, Y. Lei: International Journal of Hydrogen Energy Vol. 31 (2006), p. 517.

[15] L.M.C. Zarpelon, E. Galego, H. Takiishi, R.N. Faria: Materials Research Vol. 11 (1) (2008), p.17

[16] J.C.S. Casini, Z. Guo, H.K Liu, R.N. Faria, H. Takiishi: Batteries Vol. 1. (2015), p. 3.

[17] L.M.C. Zarpelon, R.N. Faria: Materials Science Forum Vol. 802 (2014), p. 421.

[18] J.C.S. Casini, Z.Guo, H.K Liu, E.A.Ferreira, R.N. Faria, H. Takiishi; Transactions of Nonferrous Metals Society of China Vol. 25 (2015), p. 520.